Hindawi Publishing Corporation
International Journal of Antennas and Propagation
Volume 2008, Article ID 129584, 11 pages
doi:10.1155/2008/129584

Research Article

Single and Multiple Scattering in UWB Bicone Arrays

Raffaele D'Errico[1,2] and Alain Sibille[1]

[1] *ENSTA, 32 Boulevard Victor, 75739 Paris Cedex 15, France*
[2] *DEIS, Facoltà di Ingegneria, Via del Risorgimento 2, 40100 Bologna, Italy*

Correspondence should be addressed to Raffaele D'Errico, raffaele.derrico@ensta.fr

Received 1 May 2007; Revised 12 September 2007; Accepted 29 December 2007

Recommended by Dejan Filipovic

An analysis of interactions between radiators in a UWB biconical array, drawing attention to single and multiple scatterings, is carried out. The complementarity between electrical coupling and radiation scattering is argued. The point source approximation is discussed and shown to be insufficient. An approximation of radiation scattering based on angular averaging of the scattering coefficient is proposed. This approach yields a reduction of the problem complexity, which is especially interesting in UWB multiple antenna systems, because of the large bandwidth. Multiple scattering between radiators is shown to be a second-order effect. Finally, a time domain approach is used in order to investigate pulse distortion and quantify the exactness of the proposed scattering model.

1. INTRODUCTION

It is well known that multiple antenna system (MAS) offers attractive applications in wireless communications by means of MIMO techniques that give out high channel capacities, by taking benefit of antenna diversity at both ends of the link. Furthermore, ranging applications may take advantage from MAS, through direction-of-arrival (DOA) estimation in addition to time of arrival (TOA). The same MAS principles can be applied to UWB technologies [1], in order to improve the link robustness or range, and exploit the high-multipath resolution.

Usually, arrays should be compact in order to be incorporated in radio devices. Obviously, by reducing the single antenna size or the inter-antennas distance, it is possible to minimize the overall system dimension. On the other hand, the mutual coupling also increases for closely spaced sensors, which can detrimentally modify the system performances. Thus, radiation, phase, and distortion characteristics of the single radiator are altered because of the presence of other antennas. In the case of narrow-band arrays, the theory of active element factor accounts for mutual coupling effects, including the possibility of scan blindness [2, 3]. In UWB systems, these phenomena are more difficult to investigate since the driven and the parasitic radiators act in a different way according to the frequency. Moreover, the electrical distance between the antennas depends on the wavelength. Hence, the frequency dependence is an additional parameter which introduces a supplementary complexity with respect to the traditional narrow-band systems.

Investigations on UWB arrays [4–6], often neglect coupling effects. Time-domain factor [6] frequently employed for UWB impulse radio system should be a useful mathematic tool, but it does not take into account that the single element radiation characteristics are altered when placed within a MAS.

Parametric studies on scan impedance and mutual impedance in UWB arrays have been presented in literature [7, 8]. Recently, pulse distortion introduced by interelements interaction has been studied for a particular UWB array [9], and a time-domain approach has been used to investigate the pulse distortion due to the antenna coupling [10].

In this paper, we present a general method, based on the definition of a scattering coefficient, to predict the effects of the passive radiators within MAS. The method has the advantage to avoid the use of a full method of moments (MoM) computation of the array.

In Section 2, we present an electrical circuit analysis of MAS carried out in the frequency domain, by distinguishing between coupling and *scattering* effects. Point source approximation is discussed in Section 3. In Section 4, we model the parasitic antennas as scatters, by means of antenna cross

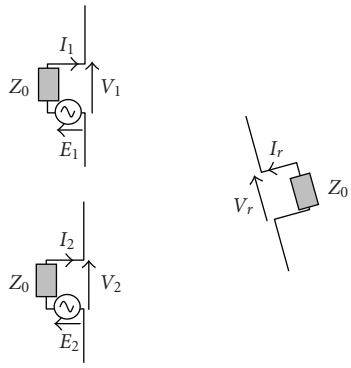

Figure 1: Multiple antennas operating in transmission.

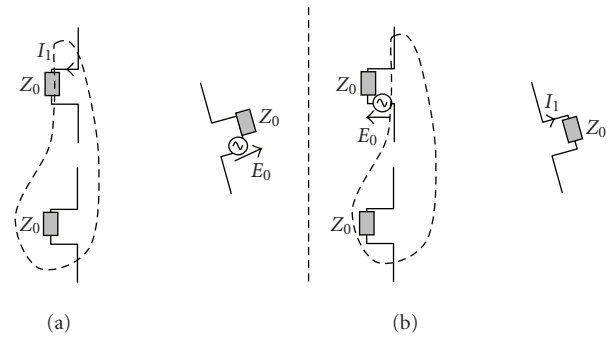

Figure 2: (a) MAS operating in reception and (b) single antenna in reception.

section. We focus on linear and circular arrays using UWB biconical antenna as simple radiator. Multiple scattering is discussed and is shown to be a second-order effect in Section 5. In Section 6, impulse distortion due to interelements interaction is discussed.

2. AN ELECTRICAL NETWORK ANALYSIS OF MULTIPLE ANTENNAS SYSTEMS

The understanding of multiple antenna systems operation is here based on electromagnetic theory and electrical networks analysis as follows. All voltages, impedances, and currents are frequency dependent. This dependence can not be neglected in UWB multiple antennas. Let us consider a MAS operating in transmission, with several source signals and impedance loads on the antenna access port, as depicted in Figure 1. We indicate with the index i ($i = 1, 2, \ldots, N$) the ith element of the transmitting array and with r a receiving antenna.

Then, at a given frequency, the system should be described by a $(N + 1) \times (N + 1)$ network complex matrix, where N is the number of antennas composing the transmitting MAS. For simplicity of discussion, let us consider $N = 2$.

$$\begin{pmatrix} E_1 - Z_0 I_1 \\ E_2 - Z_0 I_2 \\ V_r \end{pmatrix} = \begin{pmatrix} V_1 \\ V_2 \\ -Z_0 I_r \end{pmatrix} = \begin{pmatrix} Z_{11} & Z_{12} & Z_{13} \\ Z_{21} & Z_{22} & Z_{23} \\ Z_{31} & Z_{32} & Z_{33} \end{pmatrix} \begin{pmatrix} I_1 \\ I_2 \\ I_r \end{pmatrix}. \quad (1)$$

Through the superposition theorem, it is clear that a voltage V_r at the receiving port can be obtained by summing the received voltages, when V_1 has its nominal value and $V_2 = 0$, and when V_2 has its nominal value and $V_1 = 0$. Thus, in order to obtain V_r, it is sufficient to have the knowledge of as many complex radiation patterns as antenna ports, where each pattern requires 1 V applied to one port, and 0 V (short circuit) on the others. The values of V_1 and V_2 are simply obtained by solving the electrical network equations of the array in transmission, given its load and source voltage conditions.

Furthermore, by neglecting couplingbetween transmitting and receiving antennas, (1) can be simplified as

$$\begin{pmatrix} E_1 - Z_0 I_1 \\ E_2 - Z_0 I_2 \end{pmatrix} = \begin{pmatrix} V_1 \\ V_2 \end{pmatrix} = \begin{pmatrix} Z_{11} & Z_{12} \\ Z_{21} & Z_{22} \end{pmatrix} \begin{pmatrix} I_1 \\ I_2 \end{pmatrix}. \quad (2)$$

When the MAS operates in reception, the theorem of reciprocity (see Figure 2) makes it straightforward to obtain the received voltage over the loads of the array ports. Since the left and right situations are reciprocal, the current in the load of array port 1 (a) is equal to the current in the load of the single antenna (b). The second array port and its load can be considered to be part of a unique port big antenna. Thus, I_1 in the receiving array can be obtained from the knowledge of the array operating in transmission. Of course, what applies to port 1 applies to port 2 as well, so that both I_1 and I_2 in the receiving array can be computed from the complex gain patterns in transmission. The computation of I_1 requires to solve the electrical network equations to obtain the voltages on each antenna port when array port one is fed with E_0. The same work must be done again when E_0 feeds array port 2. It is important to note here that the conventions for currents signs should be properly defined.

Let us consider a two-antenna system with an ideal voltage source on port 1, a Z_0 load on port 2 ($E_2 = 0$), and the receiving antenna is load with Z_r. It is very easy to obtain

$$\begin{aligned} E_1 &= \left(Z_{11} - \frac{Z_{12}^2}{(Z_{22} + Z_0)}\right) I_1, \\ I_r &= -\left(\frac{Z_{31}}{Z_{33} + Z_r} + \frac{Z_{32} \cdot Z_{12}}{(Z_{33} + Z_r)\,(Z_{22} + Z_0)}\right) I_1. \end{aligned} \quad (3)$$

The last equation means that the received signal is equal to the sum of two terms: the first is the received signal due to the feeding of port 1 in the presence of port 2 open circuited; the second is the received signal due to the current excited in port 2, due to the finite load Z_0 and to the impedance coupling term Z_{12}, which causes radiation by antenna 2. Coming back to the general equations of the three-antennas system, we have

$$-(Z_{33} + Z_r) \cdot I_r = Z_{31} \cdot I_1 + Z_{32} \cdot I_2, \quad (4)$$

where Z_{33} is the receiving antenna self-impedance. What is very interesting in this expression is that it shows that the received signal is the superposition of 2 terms: the first is due to antenna 1 excited by a current I_1 *in the presence of antenna 2 with port 2 open circuited*, and the second is the equivalent of that by inverting indexes 1 and 2. In other words, we can very

rigorously compute the array effect on an excited element as follows.

(i) Compute the radiation with one element excited and all others open circuited.
(ii) Successively compute the radiation of each other element, *in the presence of all others open circuited*, due to the current which feeds it by proximity coupling from the first element. This current is obtained from the electrical coupling network equation.
(iii) Compute the sum of all received signals (as many ones as elements in the array).

Usually, an open-circuited element provides little electromagnetic perturbation on the other elements. This is due to the fact that a little current develops in such an element (take as an example, a quarter wavelength monopole, which is nonresonant when open circuited). Thus, the shadowing effect is very weak in this case. Neglecting this contribution is the so called *point source approximation* [11], since only secondary currents induced by coupling are responsible for radiation by the neighbouring elements.

However, if the element has a large size, current can develop along it, producing scattered radiation which we call *scattering* or diffraction, even if it is open circuited. This effect adds to the secondary radiation due to coupling.

This approach precisely defines what is meant by *scattering* and what is meant by *coupling*.

3. ANTENNA POINT SOURCE APPROXIMATION

A nonspecific isolated antenna radiates an electric field that can be written as follows:

$$\vec{E}_{\text{iso}}(r,\theta,\phi,f) = -j\eta\frac{e^{-j\beta r}}{2\pi r}\vec{E}_0(\theta,\phi,f) = K(f,r)\cdot Z_{11\,\text{iso}}(f)\cdot I_{1\,\text{iso}}(f)\cdot\vec{e}_{\text{iso}}(\theta,\phi,f), \tag{5}$$

where I_1 and Z_{11} represent, respectively, the current and self-impedance at antenna port, and K is a constant depending on the free space impedance η, the observation distance r, and the wave vector in free space β. The dependence on the frequency f is now explicit. Let us consider the $N \times N$ linear system $[V(f)] = [Z(f)][I(f)]$, where N is the number of antennas in the array. By imposing that, one antenna is fed ($V_i = 1\,\text{V}$), and other ones are terminated with their loads; it is possible to calculate the currents developed at the ports of each antenna. Then, the point source approximation of the radiated field, when the ith antenna is fed and other ones are loaded with 50 Ohms in a linear array, is

$$\vec{E}_{r_i}(r,\theta,\varphi,f) = K(f,r)\cdot Z_{11\,\text{iso}}(f)\cdot\left[I_i(f) + \sum_{\substack{n=1\\ n\neq i}}^{N} I_n(f)e^{j\Delta_n(f)}\right]\cdot\vec{e}_{\text{iso}}(\theta,\phi,f), \tag{6}$$

where $\Delta_n(f) = \text{nd}\cdot(2\pi f/c)\hat{a}\bullet\hat{r}$, d is the inter-antennas distance, $\hat{a}$ is the antennas alignment direction, and c the free space velocity. By means of this approximation, the only information that one has to know is the radiation pattern and return loss of the simple radiator, and the $N \times N$ impedance matrix of the system. No explicit near field information is needed, which has the advantage of a much simpler way to predict the multiple antenna system behavior. In a thin dipole MAS, the current distribution on the open-circuited dipole, when another one is fed, is very small; thus the scattering effect does not affect the radiation characteristics in a significant way. Let us consider two thin dipoles (radius $a = 0.1\,\text{mm}$) resonant at 3 GHz in a linear end-fire array configuration ($d = 50\,\text{mm}$). In Figure 3, we compare the radiation pattern, when the second antenna is loaded with 50 Ohms (black line), calculated by the MoM, and the radiation pattern obtained by point source approximation which neglects *scattering* effects (blue line).

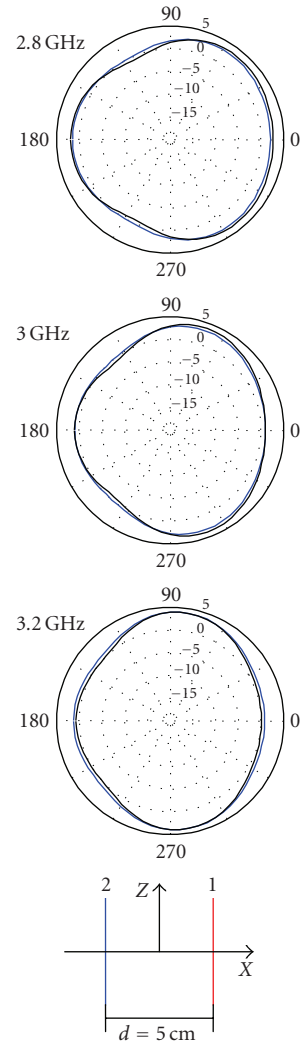

FIGURE 3: Thin dipoles ($d = 50\,\text{mm}$): simulated expected radiation pattern (black line) and point source approximation (blue line).

Accordingly, the point source approximation is satisfactory even in case of strong mutual coupling in classical narrowband systems, where dipole is commonly assumed as single radiator.

Let us employ a biconical omnidirectional antenna as simple radiator in order to investigate UWB multiple antennas.

This antenna is derived from a previous work on the design of an UWB antenna for channel measurements [12]. Antenna dimensions are 31 mm × 37 mm (diameter × height), and its input bandwidth is 2.75–16 GHz; see Figure 4. The inter-antennas distance d is taken with respect to the bicone's evolution axis.

In Figure 5, we show the azimuth radiation pattern of two bicone antennas ($d = 50$ mm), one driven and the other one loaded with 50 Ohms, together with its point source approximation. It is easy to see that the approximation does not agree with the expected radiation pattern. This is due to the fact that, when the first antenna is excited, the current density on the second open-circuited antenna is stronger than that in the dipole case, and the *scattering* effect is predominant over the coupling one. By increasing the inter-antennas distance, radiator interactions become less significant, and also *scattering*.

4. SINGLE SCATTERING BETWEEN RADIATORS

As seen in the previous section, predicting scattering turns out is essential to calculate the radiation pattern of multiple antennas, especially in UWB applications as the antenna size is not negligible with respect to the wavelength. Let us consider the same two biconical antenna arrays as above, where open circuit conditions are imposed on the second antenna port. We consider that the total radiated field is due to the sum of two contributions: the first is the suitably delayed field of the excited isolated radiator; the second, which represents the open-circuited antenna, is the same radiated field suitably delayed and multiplied by a scattering coefficient $\mathrm{SC}(f, d, \theta, \varphi)$. In a two-antenna array, as depicted in Figure 4, this results for the field radiated by the array in the expression:

$$\begin{aligned}\vec{E}\,(r,\theta,\phi,f,d) &= \vec{E}_{\mathrm{iso}}(r,\vartheta,\phi,f)\\ &\quad\cdot\left(e^{j(d\pi f/c)\sin\theta\cos\phi} + \mathrm{SC}(f,d,\theta,\phi)\cdot e^{-j(d\pi f/c)\sin\theta\cos\phi}\right).\end{aligned} \tag{7}$$

At this stage, there is no assumption as long as SC is a free parameter. The formula is just shaped in order to envision the open-circuited antenna as a scatter, which has same geometry and physical characteristics as a single element. Antennas have two possible modes of scattering: the first is the scattering due to the fact that the antenna is of a given shape, material and size; the second because the antennas have been designed to transmit or receive RF energy at the relevant frequency [13]. By means of a MoM tool (Wipl-D), it is possible to compute the antenna radar cross section and scattered field Es by the open circuited antenna, illuminated by a field Ei of a plane wave incident from the direction (θ_i, ϕ_i), where the excited radiator is located in the array. We here limit ourselves to the main polarization, that is, the θ-component. Once the scattered field by the open-circuited antenna has been computed by MoM, the scattering coefficient SC can be approximated for every distance as follows:

$$\mathrm{SC}(f,d,\theta,\phi) \approx \frac{1}{d}e^{-j(2\pi f/c)d}\frac{E_s(\theta,\phi,f)}{E_i(\theta_i,\phi_i,f)}. \tag{8}$$

Thus, the scattering coefficient is approximated by a far field computation, which is easier than a near field computation. In Figure 6, we show the result of this SC approximation on the computation of the azimuth radiation pattern. We observe a varying accuracy according to the frequency; nevertheless the approximation is satisfactory even at low inter-antennas distance ($d = 50$ mm). Naturally, the discrepancy increases at the higher frequencies, as the wavelength becomes smaller than the radiator size. Using (7) and by knowing the exact value of $\vec{E}\,(r,\theta,\varphi,f,d)$ and $\vec{E}_{\mathrm{iso}}(r,\theta,\varphi,f)$, one can also obtain the exact value of the SC.

Looking at the cylindrical antenna geometry, a natural but strong approximation is to eliminate the ϕ-dependency. Averaging over the azimuth angle will introduce an inaccuracy in evaluating the SC and consequently also on the radiation pattern. In Figures 7 and 8, we compare the azimuth-averaged exact value of SC with that computed with (8). A good agreement is shown for all frequencies and elevation angles, with the exception of the lowest frequencies at the zenith (z-axis). This should in part be explained by the presence of a stronger side component of the scattered field, which is not taken into account in the plane wave approximation. Furthermore, it is interesting to see that from 10 to 16 GHz the antenna presents a different scattering behavior in amplitude as well in phase. This is due to the fact that an UWB antenna, even if matched, does not present the same radiation behavior over its full bandwidth. In particular, this bicone was designed for channel measurement in the FCC band, that is, below 10.6 GHz [12].

Obviously, using a mean value in the azimuth dependence of the SC yields an inaccuracy in the radiation pattern computation, but it is interesting to observe (see Figure 9) that this inaccuracy may be tolerable. In particular, when the antennas are distant enough, the error introduced by averaging can be neglected as depicted in Figure 9. This allows a reduction of the problem complexity, and a reduction of the number of parameters needed to describe the multiple antennas behavior, which has some virtues due the large bandwidth in UWB. In Figures 10 and 11, we show the expected radiation pattern together with its scattering approximation on two elevation planes. The SC model is less accurate on the X-Z plane (see Figure 10) than on Y-Z plane (see Figure 11) where the array effect is more significant.

The two antennas array presented above is a simple case of interaction between radiators, where the parasitic element can be easily modeled as a scatter.

Let us now consider a circular array, as depicted in Figure 12 (radius $a = 50$ mm), composed by three equally spaced bicone antennas. The driven radiator (antenna 1) is

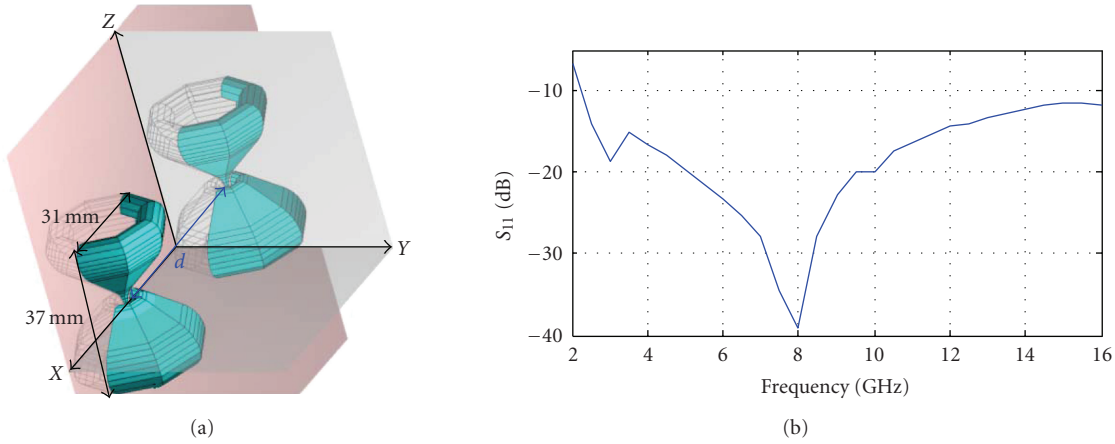

(a) (b)

FIGURE 4: (a) ENSTA bicone antennas and (b) ENSTA bicone return loss.

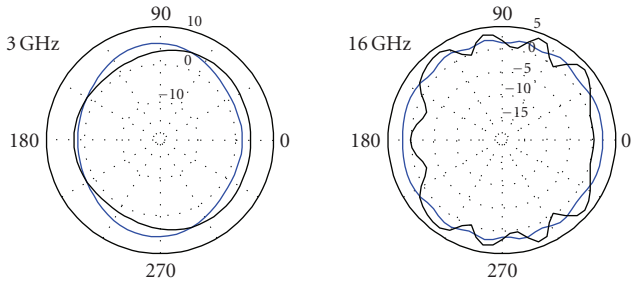

(a) (b)

FIGURE 5: Two ENSTA bicone antennas ($d = 50$ mm): antenna 1 is excited; antenna 2 is 50 Ohms loaded. Simulated expected radiation pattern (black line) and point source approximation (blue line).

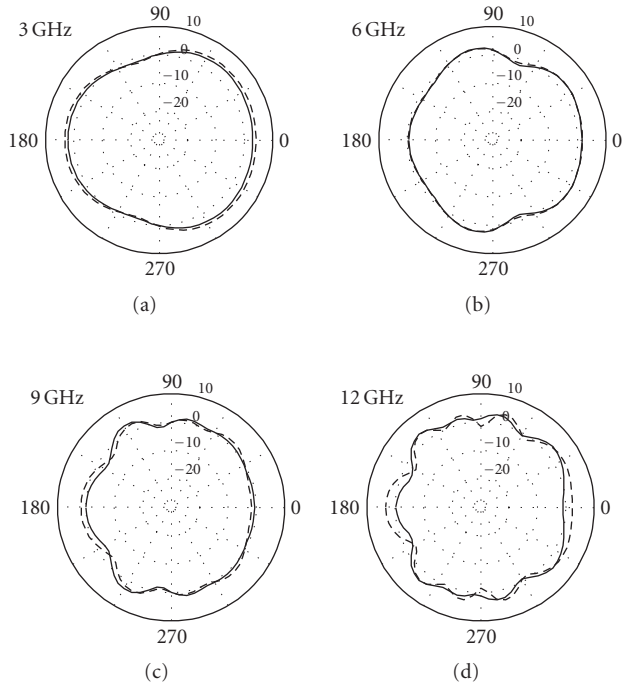

(a) (b) (c) (d)

FIGURE 6: Expected azimuth (X-Y plane) radiation pattern for two antennas (solid line) and SC approximation (dashed line). Antenna 1 is excited; antenna 2 is open circuited ($d = 50$ mm).

placed along the y-axis, while the others are open circuited. This is a generalization of the two bicones array presented above. Thus, the total radiated field can be expressed as

$$\vec{E}(r,\theta,\phi,f,d) = \vec{E}_{\text{iso}}(r,\theta,\phi,f) \cdot \left(e^{j(2\pi/\lambda)a\sin\theta\cos(\phi-\phi_1)} + \sum_{n=2}^{N} \text{SC}_{n1}(f,d,\theta,\phi)\cdot e^{j(2\pi/\lambda)a\sin\theta\cos(\phi-\phi_n)}\right), \quad (9)$$

where φ_n represents the azimuth position of the nth radiator, and $\text{SC}_{n1}(f,d,\theta,\varphi)$ is the scattering coefficient calculated by (8), but properly turned in order to take into account the nth antenna position with respect to the fed antenna. Hence, we consider only the scattered field by antennas 2 and 3 due to the excitation of antenna 1. Multiple scattering between the two open-circuited antennas is here neglected. Figure 12 shows that effectively multiple scattering should be neglected without a significant degradation of the approximation accuracy.

5. MULTIPLE SCATTERING BETWEEN RADIATORS

Generally, by increasing the number of antennas, multiple scattering effects have to be taken into account. However, depending on the array configuration this can be assumed as a second-order effect.

Let us consider a three bicones linear array along the x-axis: antenna 1 is placed at $x = d$, antenna 2 at $x = 0$, and antenna 3 at $x = -d$.

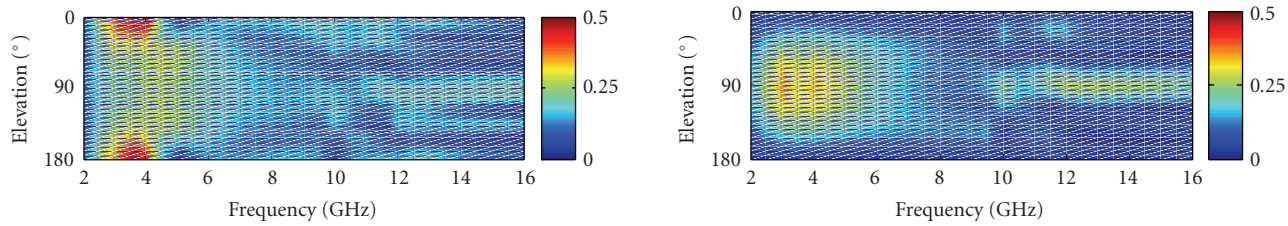

Figure 7: Azimuth-averaged SC modulus of ENSTA bicone antenna ($d = 50$ mm): (a) exact computation and (b) computation by means of scattered fields.

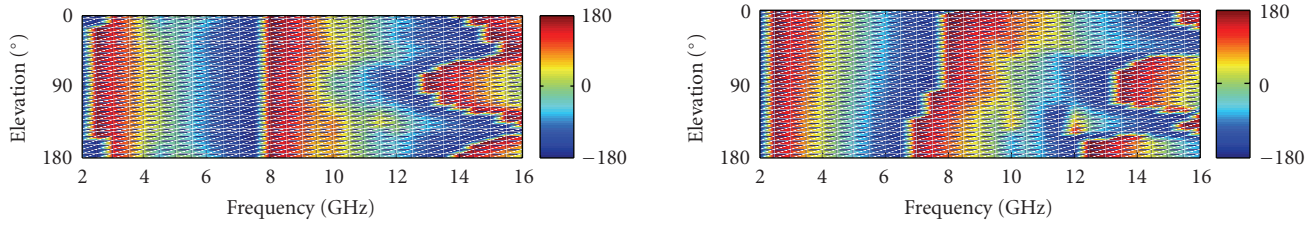

Figure 8: Azimuth-averaged SC argument of ENSTA bicone antenna ($d = 50$ mm): (a) exact computation and (b) computation by means of scattered field.

When the antenna 1 is fed, single and multiple scatterings should be considered. According to (7) and (8), the scattered field by antenna 2 can be computed as

$$\vec{E}_{\text{open }21}(r,\theta,\phi,f,d) = \vec{E}_{\text{iso}}(r,\theta,\phi,f)\cdot \text{SC}_{21}(f,d,\theta,\phi), \tag{10}$$

and the scattered field by antenna 3 can be expressed as

$$\vec{E}_{\text{open }31}(r,\theta,\phi,f,d) = \vec{E}_{\text{iso}}(r,\theta,\phi,f)\cdot\left(\text{SC}_{31}(f,d,\theta,\phi)\cdot e^{-j(2d\pi f/c)\sin\theta\cos\phi}\right). \tag{11}$$

Scattering coefficients are computed according to (8):

$$\begin{aligned}\text{SC}_{31}(f,d,\theta,\phi) &\approx \frac{1}{2\cdot d}e^{-j(2\pi f/c)2\cdot d}\frac{E_s(\theta,\phi,f)}{E_i(\theta_{31},\phi_{31},f)},\\ \text{SC}_{21}(f,d,\theta,\phi) &\approx \frac{1}{d}e^{-j(2\pi f/c)d}\frac{E_s(\theta,\phi,f)}{E_i(\theta_{21},\phi_{21},f)}.\end{aligned} \tag{12}$$

In addition, multiple scattering between antenna 2 and antenna 3, which are open circuited, can be expressed as

$$\vec{E}_{\text{open }32}(r,\theta,\phi,f,d) = \vec{E}_{\text{iso}}(r,\theta,\phi,f)\cdot\text{SC}_{21}(f,d,\theta,\phi)\cdot\left(\text{SC}_{32}(f,d,\theta,\phi)\cdot e^{-j(2d\pi f/c)\cos\theta\cos\phi}\right), \tag{13}$$

where

$$\text{SC}_{32}(f,d,\theta,\phi) \approx \frac{1}{d}e^{-j(2\pi f/c)d}\frac{E_s(\theta,\phi,f)}{E_i(\theta_{32},\phi_{32},f)}. \tag{14}$$

In (10), (11), and (13), electric fields are opportunely delayed by taking into account the antenna position along the x-axis of different antennas. According to (8), the scattering coefficients in (12), and (14) are computed by simulating the single antenna cross section. In the computation of a generic SC_{mn}, the illuminating radiated field is a plane wave, coming from the direction (θ_{mn},ϕ_{mn}) of the mth antenna with respect to the nth antenna. Practically, it is the same scattering coefficient in (8), but suitably attenuated, delayed, and oriented, in order to take into account the position of the antennas within the array. Finally, the total radiated electric field can be computed by means of the superposition theorem as

$$\begin{aligned}\vec{E}\,(r,\theta,\phi,f,d) = {}& \vec{E}_{\text{iso}}(r,\theta,\phi,f)e^{j(2d\pi f/c)\sin\theta\cos\phi}\\ &+ \vec{E}_{\text{open }21} + \vec{E}_{\text{open }31} + \vec{E}_{\text{open }32}.\end{aligned} \tag{15}$$

This expression neglects the 2nd-order scattered field by the fed antenna due to the scattered fields by both antenna 2 and antenna 3. In Figures 13 and 14, we show the expected radiation pattern (black line) and the electric field computed by means of (15), (blue marker) for two different inter-antennas distance $d = 5$ cm and $d = 10$ cm. The electric field agrees quite well with the expected radiation pattern especially at higher inter-antennas distance. However, multiple scattering expressed in (14) is small comparing to the single scattering terms, given that a little current distribution is developed on open-circuited antenna 2.

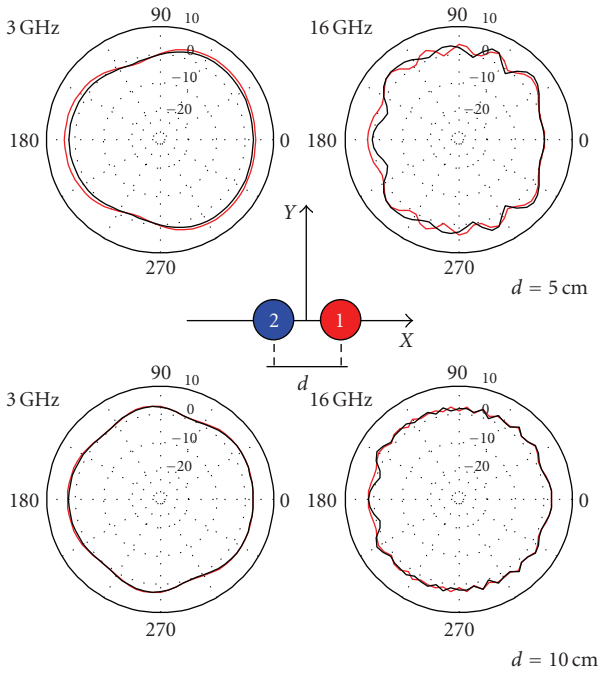

FIGURE 9: Expected azimuth (X-Y plane) radiation pattern for two antennas (solid line); SC approximation (red line) with scattering coefficient averaged over the azimuth angle. Antenna 1 is excited; antenna 2 is open circuited.

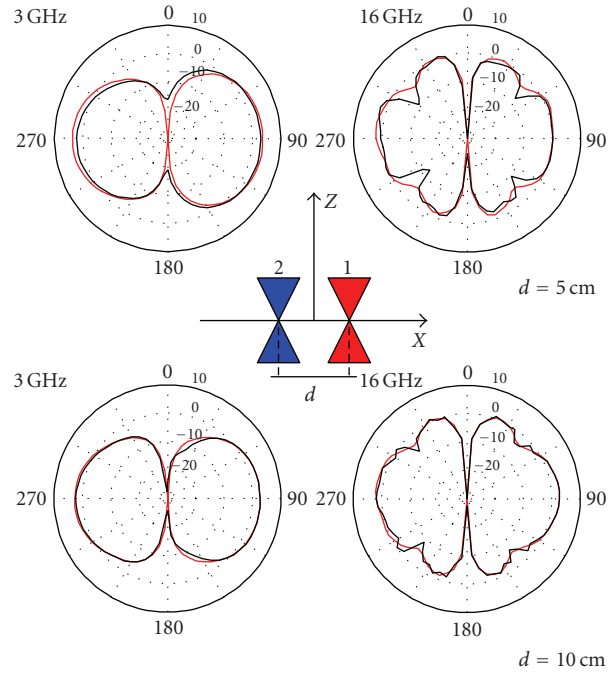

FIGURE 10: Expected radiation pattern in elevation ($\varphi = 0°$, Z-X plane) (black line) and SC azimuth-averaged approximation (red line). Antenna 1 is excited; antenna 2 is open circuited.

Furthermore, the single scattering by antenna 3, computed by means of (11) should be neglected because of the shadowing due to the presence of antenna 2.

Consequently, the total radiated electric field can be very simply approximated as

$$\vec{E}\,(r,\theta,\phi,f,d) = \vec{E}_{\text{iso}}(r,\theta,\phi,f)e^{j(2d\pi f/c)\sin\theta\cos\phi} + \vec{E}_{\text{open }21}. \tag{16}$$

Figures 13 and 14 validate this assumption by showing that the radiation pattern computed by means of (16) is nearly exactly superimposed to the radiation pattern computed by means of (15), which takes into account all the single and multiple scattering terms. This means that, in this case, the three bicones array has the same behavior as the two bicones array.

Similarly, when antenna 2 is fed, only single scattering on antennas 1 and 3 can be taken into account. Thus, the total radiated field can be written as

$$\begin{aligned}\vec{E}_{\text{open}}(r,\theta,\phi,f,d) &= \vec{E}_{\text{iso}}(r,\theta,\phi,f)\cdot\Big(1+\text{SC}_{12}(f,d,\theta,\phi)\cdot e^{j(2d\pi f/c)\sin\theta\cos\phi} \\ &\quad + \text{SC}_{32}(f,d,\theta,\phi)\cdot e^{-j(2d\pi f/c)\sin\theta\cos\phi}\Big),\end{aligned} \tag{17}$$

where $\text{SC}_{12}(f,d,\theta,\varphi)$ and $\text{SC}_{32}(f,d,\theta,\varphi)$ are the scattering coefficients for antennas 1 and 3 calculated by (8), by taking into account their position with respect to the fed antenna. Figure 15 shows the azimuth pattern together with its SC approximation for a linear array, when the central antenna is fed and expressed in (17). Multiple scattering between two open-circuited antennas can be neglected while preserving the approximation accuracy.

The model taking into account single and double scatterings, between two parasitic elements, can be generalized for a nonspecific N antennas array. Thus, the radiated field by the mth fed element, within the array, can be written as

$$\begin{aligned}&\vec{E}_m(r,\theta,\phi,f,d) \\ &\quad = \vec{E}_{\text{iso}}(r,\theta,\phi,f) \\ &\qquad \cdot\left(e^{j\delta_m(f)} + \sum_{\substack{n=1\\n\neq m}}^{N}\left(\text{SC}_{nm} + \sum_{\substack{p=1\\p\neq n}}^{N}(\text{SC}_{np}\cdot\text{SC}_{pm})\right)e^{j\delta_n(f)}\right),\end{aligned} \tag{18}$$

where SC_{nm} is the scattering coefficient between the nth and mth antenna computed by means of (8), omitting the (f,d,θ,ϕ) dependence for the sake of briefness. The phase delay $\delta_n(f) = (2\pi f/c)\vec{a}_n\bullet\hat{r}$ takes into account the position of the nth antenna (indicated by the vector $\vec{a}_n$) in the array. As far as double scattering can be considered as a second-order effect, (18) can be simplified as

$$\vec{E}_m(r,\theta,\phi,f,d) = \vec{E}_{\text{iso}}(r,\theta,\phi,f)\cdot\left(e^{j\delta_m(f)} + \sum_{\substack{n=1\\n\neq m}}^{N}\text{SC}_{nm}e^{j\delta_n(f)}\right). \tag{19}$$

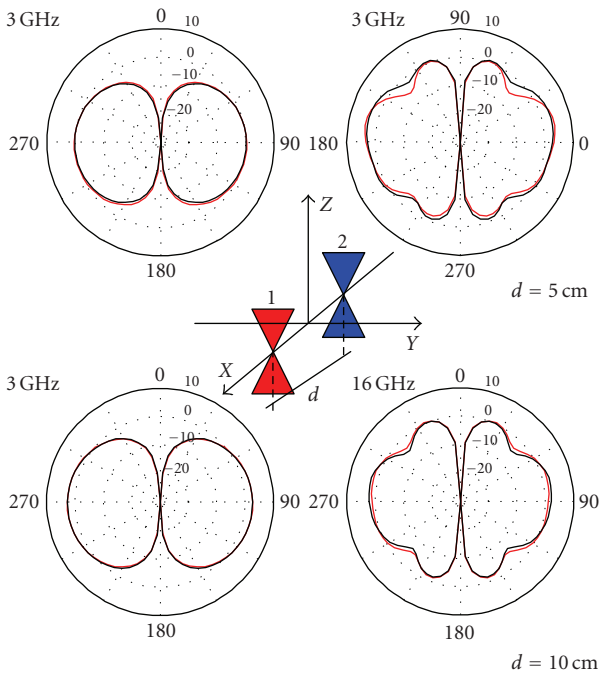

Figure 11: Expected radiation pattern in elevation ($\varphi = 90^\circ$, Z-Y plane) (black line) and SC azimuth-averaged approximation (red line). Antenna 1 is excited; antenna 2 is open circuited.

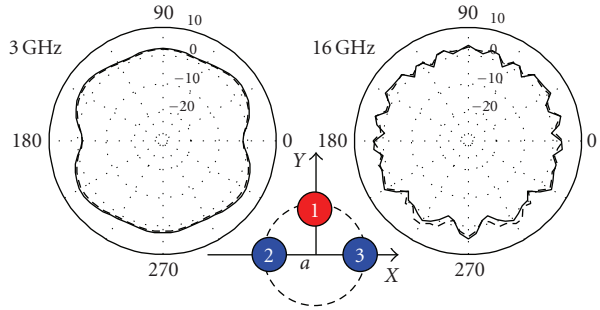

Figure 12: Three-bicone circular array with feeding on antenna 1 and open-circuit on antennas 2 and 3. Expected azimuth (X-Y plane) radiation pattern (solid line) and SC approximation (dot line).

Therefore, once the single isolated antenna radiation and its antenna cross section have been computed, one should easily predict the performances of a generic array. The proposed approach is of particular interest in compact MAS design, for which the radiation pattern distortion is stronger. On the other hand, the proposed model is still useful in large bidimensional arrays, but multiple scattering should be considered, given that mutual coupling can generate phase resonance among the arrays [14].

6. PULSE DISTORTION DUE TO INTER-ELEMENT INTERACTION

By means of time domain approach, it is possible to access the waveform of the radiated field as a function of the angular coordinates. When an antenna is excited by an incident signal $w(t)$, it radiates an electric field, whose waveform, $e(\theta, \phi, t)$ in the (θ, ϕ) direction, is a distorted version of the incident one. Distortion is due to dispersion, that is, the frequency-dependence of the realized gain and the angular frequency-deviation of the radiation pattern. A common feature in UWB antenna characterization is a time domain approach with the purpose to characterize the distortion introduced by the antenna. In multiple antenna systems, the additional distortion due to the interaction between radiators has to be taken into account. Even when close antennas are open circuited, scattering effects are responsible for some distortion, which is the time domain counterpart of the alteration of the radiation pattern discussed in the previous paragraphs. This is of practical importance in pulsed schemes, where distortion may affect the overall system performance by introducing inter-symbol interference.

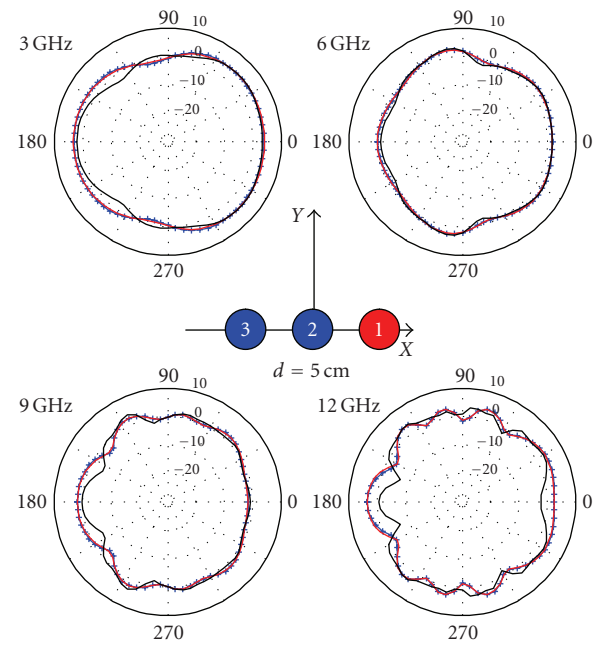

Figure 13: Three-bicone linear array ($d = 5$ cm) with feeding on antenna 1 and open circuit on antennas 2 and 3. Expected azimuth (X-Y plane) radiation pattern (black line), SC approximation with all single and multiple scattering terms (blue marker), and SC approximation with only single scattering on antenna 2 (red line).

Here, the chosen excitation signal $w(t)$ is a Gaussian impulse with a -10 dB power bandwidth of 3–10.0 GHz (see Figure 16). Our aim is to estimate the accuracy of the SC approximation.

In Figures 17, 18, 19 we show, for different directions, the waveform $e(\theta, \phi, t)$ radiated by a biconical antenna in a two radiators linear array when the parasitic element is open circuited, and we compare it with the radiated waveform $e_{SC}(\theta, \phi, t)$ computed by means of the SC. The inter-antennas distance is 5 cm. The computed waveform agrees quite well with the expected one. A small degradation accuracy is shown for the highest elevation angles and in the end-fire direction ($\phi = 180^\circ$).

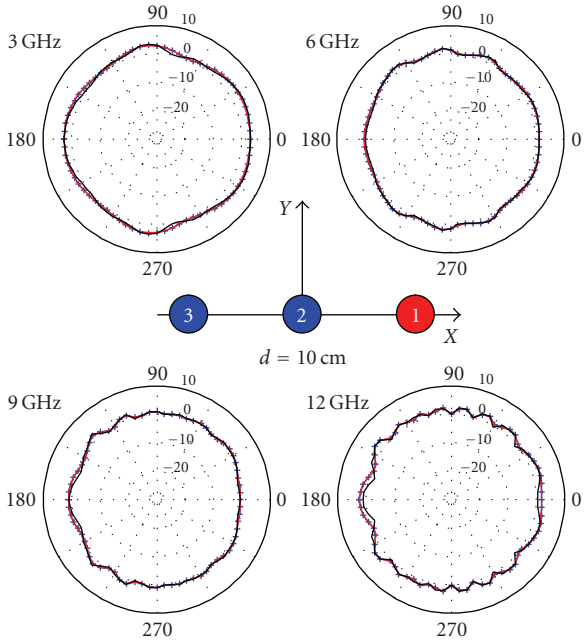

FIGURE 14: Three-bicone linear array ($d = 10$ cm) with feeding on antenna 1 and open circuit on antennas 2 and 3. Expected azimuth (X-Y plane) radiation pattern (black line), and SC approximation with all single and multiple scattering terms (blue marker), SC approximation with only single scattering on antenna 2 (red line).

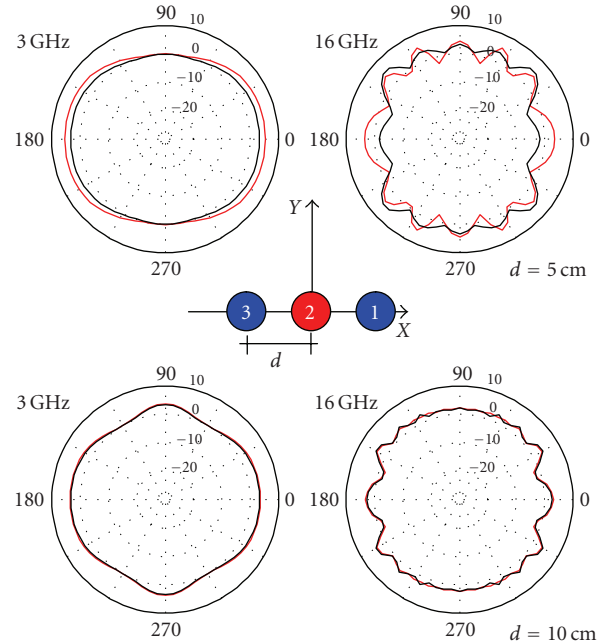

FIGURE 15: Three-bicone linear array with feeding on antenna 2 and open circuit on antennas 1 and 3. Expected azimuth (X-Y plane) radiation pattern (solid line) and SC approximation (red line).

Figures 17, 18, 19 show a visual agreement of the approximation. Let us consider a simple pulse scheme in a simple AWGN channel (power spectral density equal to N_0). The receiver is a classical correlator, and the reference template pulse is $\mathrm{ref}(t)$.

Since the receiver usually chooses $\tau_{\max}$ in order to maximize SNR, then

$$\mathrm{SNR} = \frac{\int_{-\infty}^{+\infty} |\mathrm{rec}(t)|^2 dt}{Z_0 N_0} \times \left| \frac{\int_{-\infty}^{+\infty} \mathrm{rec}(t)\mathrm{ref}(t-\tau_{\max})dt}{\sqrt{\int_{-\infty}^{+\infty} |\mathrm{rec}(t)|^2 dt} \cdot \sqrt{\int_{-\infty}^{+\infty} |\mathrm{ref}(t)|^2 dt}} \right|^2, \quad (20)$$

where Z_0 is the load on receiving antenna, and $\mathrm{rec}(t)$ is the received pulse which can be expressed as [15]

$$\mathrm{rec}(t,\theta,\phi) = \frac{\partial^{-1}}{\partial t} * h_{\mathrm{TX}}(t,\theta,\varphi) * h_{\mathrm{RX}}(t,\theta,\varphi) * w(t), \quad (21)$$

where $h_{\mathrm{TX}}(t,\theta,\varphi)$ and $h_{\mathrm{RX}}(t,\theta,\varphi)$ are the transmitting impulse response of the transmitting and receiving antennas, respectively. The reference pulse is chosen to be identical to the received pulse when two ideal isotropic antennas are used. If we consider an ideal antenna at the transmitting side and an array on the receiving side, we can estimate the effect

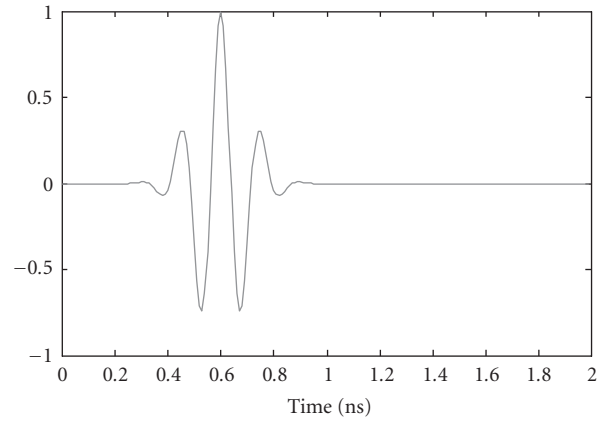

FIGURE 16: Excitation signal at antenna port: Gaussian impulse with a −10 dB power bandwidth of 3–10.0 GHz.

of the SC approximation on SNR:

$$\mathrm{SNRD}(\theta,\phi) = \frac{\mathrm{SNR}_{\mathrm{SC}}(\theta,\phi)}{\mathrm{SNR}_{\mathrm{expected}}(\theta,\phi)}, \quad (22)$$

where $\mathrm{SNR}_{\mathrm{SC}}(\theta,\varphi)$ and $\mathrm{SNR}_{\mathrm{expected}}(\theta,\varphi)$ are the SNR computed by using the SC approximated and the real antenna impulse response.

As depicted in Figure 20, the difference on SNR is less then 0.7 dB in case of low inter-antennas distance ($d = 5$ cm) and about 0 dB for higher antenna distances ($d = 10$ cm, $d = 20$ cm).

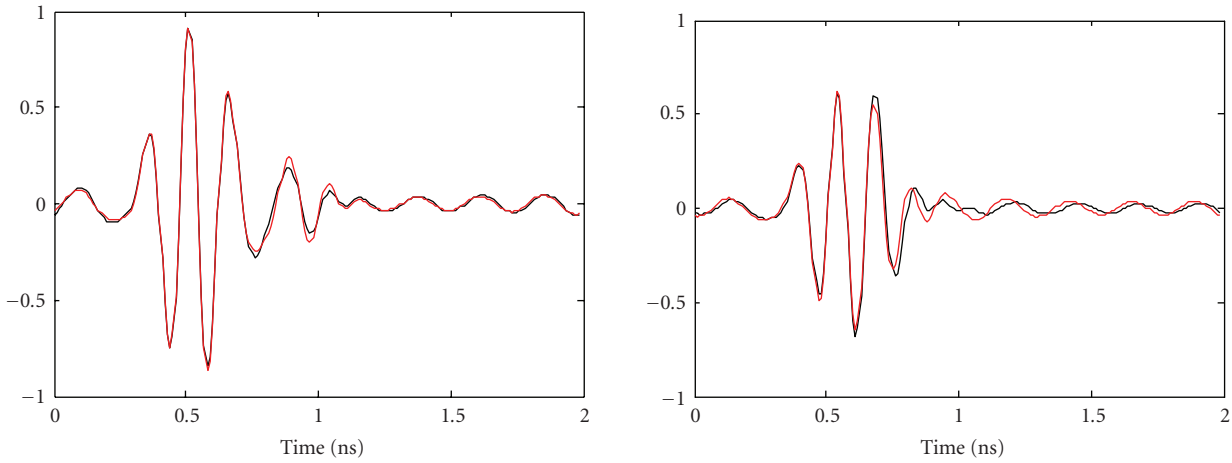

Figure 17: Expected radiated waveform (black line), SC approximation (red line) at (a) $\varphi = 0^\circ$ and $\theta = 90^\circ$, (b) $\theta = 30^\circ$.

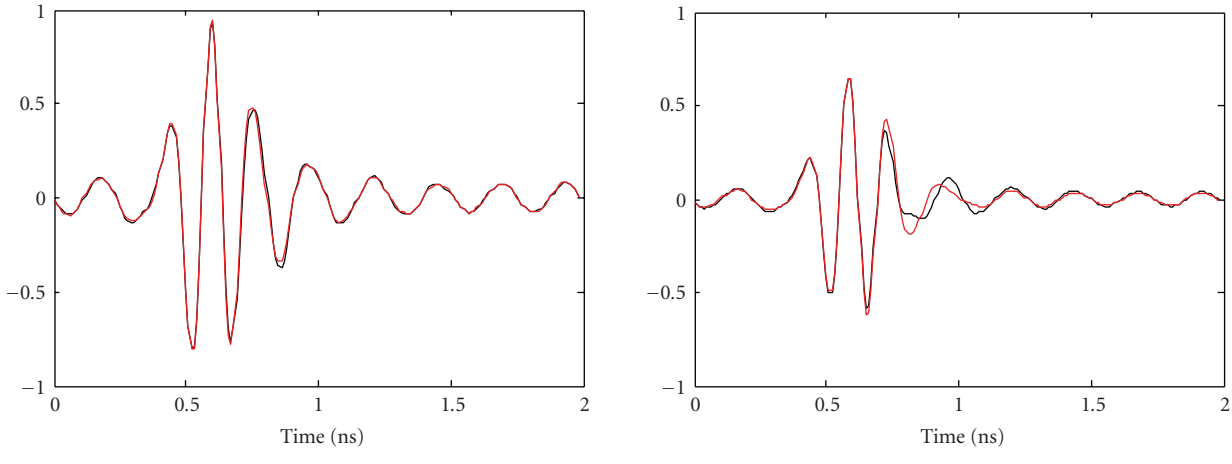

Figure 18: Expected radiated waveform (black line), SC approximation (red line) at (a) $\varphi = 90^\circ$ and $\theta = 90^\circ$, (b) $\theta = 30^\circ$.

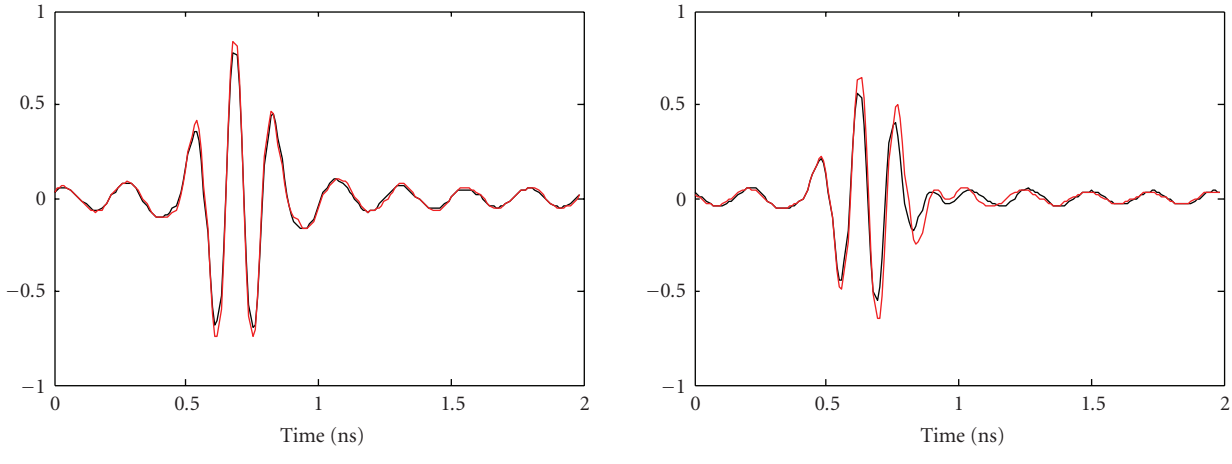

Figure 19: Expected radiated waveform (black line), SC approximation (red line) at (a) $\varphi = 180^\circ$ and $\theta = 90^\circ$, (b) $\theta = 30^\circ$.

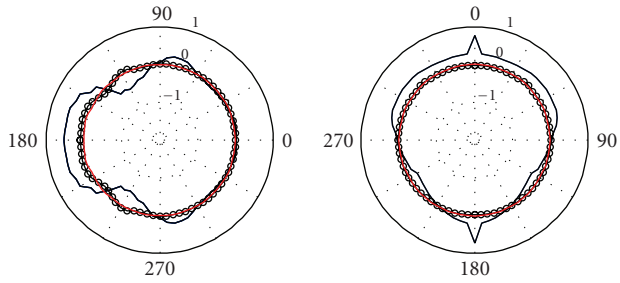

FIGURE 20: (a) SNRD (dB) in azimuth and (b) elevation plane. d = 5 cm (black line), 10 cm (open dots), and 20 cm (red line).

7. CONCLUSIONS

A network analysis of multiple antenna systems has been carried out in order to identify the origins of inter-elements interaction and model them. This approach discriminate precisely what is *scattering* from what is *coupling*. When the first one is negligible, a point source approximation may be applied, as commonly occurs with thin dipoles. In contrast with UWB antennas, which generally occupy a larger volume, the contribution to total electric field by the open-circuited elements becomes more significant. Thus, *scattering* has been modelled by a *scattering coefficient* (SC). A practical way to obtain this SC is to illuminate the open-circuited passive element and compute the bistatic antenna radar cross section. This approximation neglects the incident wave curvature and near field effects, but the reasonable agreement with full computations justifies its use, given its much greater simplicity. As a result, only single radiator pattern and SC are sufficient to predict the multiple antennas performance. The dependence on azimuth angle can further be averaged in the bicone antennas case, without significant loss in approximation validity. This means a simplification of the problem of inter-elements interaction, and a reduction of the number of parameters describing the phenomena. Multiple scattering between antennas can be considered as a second-order effect. Furthermore, single scattering can be neglected for the most distant radiators, especially if shadowing by a closer radiator occurs. As a consequence, a three bicones linear array has the same behavior as the two bicones array when the driven radiator is at the extremity. More generally, scattering due to the closest elements is the major cause of radiation pattern alteration and additional distortion. Finally, additional distortion due to inter-elements interaction has been investigated. It has been shown that the SC approximation is accurate enough to predict the effect of the antenna in an UWB pulse scheme. The generality of the proposed model simplifies the task of the antenna designer, who does not have to simulate several array designs, and, consequently, time consuming full-MoM simulations of the whole array are not required.

ACKNOWLEDGMENT

This work was in part supported by the European Commission under IST integrated project *PULSERS Phase II*.

REFERENCES

[1] A. Sibille, "Spatial diversity," in *UWB Communication Systems—A Comprehensive Overview*, EURASIP Book Series on Signal Processing and Communications, pp. 302–329, Hindawi Publishing Corporation, New York, NY, USA, 2006.

[2] D. M. Pozar, "The active element pattern," *IEEE Transactions on Antennas and Propagation*, vol. 42, no. 8, pp. 1176–1178, 1994.

[3] K. K. Chan, R. M. Turner, and K. Chadwick, "Coupling coefficients and active element patterns of finite waveguide arrays," in *Proceedings of the IEEE Antennas and Propagation Society International Symposium Digest (APS '95)*, vol. 3, pp. 1396–1399, Newport Beach, Calif, USA, June 1995.

[4] A. Shlivinski and E. Heyman, "A unified kinematic theory of transient arrays," in *Ultra-Wideband Short-Pulse Electromagnetics*, P. D. Smith and S. R. Cloude, Eds., pp. 327–334, Kluwer Academic/Plenum Publishers, New York, NY, USA, 2000.

[5] W. Soergel, C. Waldschmidt, and W. Wiesbeck, "Transient radiation from a linear UWB antenna array," in *Proceedings of the URSI International Symposium on Electromagnetic Theory (URSI EMTS '04)*, pp. 1254–1256, Pisa, Italy, May 2004.

[6] S. Foo and S. Kashyap, "Time-domain array factor for UWB antenna array," *Electronics Letters*, vol. 39, no. 18, pp. 1304–1305, 2003.

[7] T. Chio and D. H. Schaubert, "Parameter study and design of wide-band widescan dual-polarized tapered slot antenna arrays," *IEEE Transactions on Antennas and Propagation*, vol. 48, no. 6, pp. 879–886, 2000.

[8] P. L. Tokarsky, "Coupling effects in resistive UWB antenna arrays," in *Proceedings of the 3rd International Conference in Ultrawideband and Ultrashort Impulse Signals*, pp. 188–190, Sevastopol, Ukraine, September 2006.

[9] G. Kotyrba and H. J. Chaloupka, "On signal distortion in compact UWB arrays due to element interaction," in *Proceedings of the IEEE Antennas and Propagation Society International Symposium Digest (APS '05)*, vol. 1 A, pp. 614–617, Washington, DC, USA, July 2005.

[10] M. Ciattaglia and G. Marrocco, "Investigation on antenna coupling in pulsed arrays," *IEEE Transactions on Antennas and Propagation*, vol. 54, no. 3, pp. 835–843, 2006.

[11] K. Siakavara and J. N. Sahalos, "A simplification of the synthesis of parallel wire antenna arrays," *IEEE Transactions on Antennas and Propagation*, vol. 37, no. 7, pp. 936–940, 1989.

[12] H. Ghannoum, S. Bories, C. Roblin, and A. Sibille, "Biconical antennas for intrinsic characterization of the UWB channel," in *Proceedings of the IEEE International Workshop on Antenna Technology: Small Antennas and Novel Metamaterials (IWAT '05)*, vol. 2005, pp. 101–104, Singapore, March 2005.

[13] R. C. Hansen, "Relationship between antennas as scatters and as radiators," *Proceedings of the IEEE*, vol. 77, no. 5, pp. 659–662, 1989.

[14] R. W. P. King, "Supergain antennas and the Yagi and circular arrays," *IEEE Transactions on Antennas and Propagation*, vol. 37, no. 2, pp. 178–186, 1989.

[15] A. Shlivinski, E. Heyman, and R. Kastner, "Antenna characterization in the time domain," *IEEE Transactions on Antennas and Propagation*, vol. 45, no. 7, pp. 1140–1149, 1997.